Journal of Chromatography B 1179 (2021) 122861

Contents lists available at ScienceDirect

Journal of Chromatography B

journal homepage: www.elsevier.com/locate/jchromb

Radical scavenging activity and metabolomic profiling study of ylang-ylang essential oils based on high-performance thin-layer chromatography and multivariate statistical analysis

Leo Lebanov [a,b,1], Shing Chung Lam [a,1], Laura Tedone [a], Tomislav Sostaric [c], Jason A. Smith [d], Alireza Ghiasvand [a], Brett Paull [a,b,*]

[a] Australian Centre for Research on Separation Science (ACROSS), School of Natural Sciences, University of Tasmania, Hobart, TAS, Australia
[b] ARC Industrial Transformation Research Hub for Processing Advanced Lignocellulosics Products (PALs), School of Natural Sciences, University of Tasmania, Hobart, TAS, Australia
[c] Chromatech Scientific Pty Ltd, Yangebup, WA, Australia
[d] School of Natural Sciences, University of Tasmania, Hobart, TAS, Australia

ARTICLE INFO

Keywords:
Free radical scavenging activity
Ylang-ylang essential oil
Distillation grades
High performance thin layer chromatography
Multivariate statistical analysis

ABSTRACT

Ylang-ylang (YY) essential oil (EO) is distilled from the fresh-mature flowers of the Annonaceae family tropical tree *Cananga odorata* [Lam.] Hook. f. & Thomson, and is widely used in perfume and cosmetic industries for its fragrant character. Herein, two different metabolomic profiles obtained using high-performance thin-layer chromatography (HPTLC), applying different stains, namely 2,2-diphenyl-1-picrylhydrazyl (DPPH·) and *p*-anisaldehyde, were used for discrimination of 52 YY samples across geographical origins and distillation grades. The first profile is developed using the DPPH· stain based on the radical scavenging activity (RSA) of YY EOs. Results of the HPTLC-DPPH· assay confirmed that RSA of YY EOs is in proportion to the length of distillation times. Major components contributing to the RSA of YY EOs were tentatively identified as germacrene D and α-farnesene, eugenol and linalool, by gas chromatography-mass spectrometry (GC–MS) and GC-flame ionisation detector (GC-FID). The second profile was developed using the general-purpose *p*-anisaldehyde stain based on the general chemical composition of YY EOs. Untargeted metabolomic discrimination of YY EOs from different geographical origins was performed based on the HPTLC-*p*-anisaldehyde profiles, followed by principal component analysis (PCA). A discrimination and prediction model for identification of YY distillation grade was developed using PCA and partial least squares regression (PLS) based on binned HPTLC-ultraviolet (254 nm) profiles, which was successfully applied to distillation grade determination of blended YY Complete EOs.

1. Introduction

Ylang-ylang (YY) essential oil (EO) is distilled from the fresh-mature flowers of the Annonaceae family tropical tree *Cananga odorata* [Lam.] Hook. f. & Thomson [1]. Depending on the length of fractional distillation times, YY EO is usually classified into four grades, i.e. Extra (YExtra), First (YI), Second (YII), Third (YIII), which have different chemical compositions and are thus utilised for different purposes [2]. YY Complete (YCompl) is the mixture of all grades obtained in fractional distillation. With the shortest distillation time, YExtra has the highest abundance of fragrant compounds, such as *p*-cresyl methyl ether, methyl benzoate, linalool, benzyl acetate and geranyl acetate, which contribute to the fresh, floral, and slightly fruity aroma, and thus a desired product for application within the perfume and cosmetic industries [3]. Prolonging the distillation time leads to the increase of higher molecular weight and less volatile compounds in subsequent YI, YII and YIII grades, especially sesquiterpenes, such as β-caryophyllene, germacrene D and α-farnesene [2]. It has also been reported that chemical composition of YY EOs vary significantly among different geographical origins, e.g. the typical YExtra samples from Comoros showed higher levels of benzyl acetate and (*E*)-cinnamyl acetate as compared to those from Madagascar [1]. Aside from their fragrant character, it is also well known that YY EO possesses multiple bioactive compounds, delivering antibacterial, antifungal, and antioxidant activity [4]. Many EOs, due to

* Corresponding author at: School of Natural Sciences, Private Bag 75, University of Tasmania, Hobart, TAS 7001, Australia.
E-mail address: brett.paull@utas.edu.au (B. Paull).

1 Leo Lebanov and Shing Chung Lam has contributed equally to this work and claim joint first authorship of this manuscript.

https://doi.org/10.1016/j.jchromb.2021.122861
Received 19 April 2021; Received in revised form 8 June 2021; Accepted 12 July 2021
Available online 15 July 2021
1570-0232/

their strong antioxidant properties, have been added as preservatives to various food products, including vegetable oils [5], butter [6] and meat products [7]. In addition, they are regularly found in cosmeceutical and skincare products, such as facial masks and gels, which protect the skin against reactive oxygen species (ROS) [8,9].

Due to the volatile nature of EOs, gas chromatography (GC) (one- or two-dimensional) hyphenated with mass spectrometry (MS) is the most commonly used technique applied to their metabolomic studies [10–12]. However, high-performance thin-layer chromatography (HPTLC), nowadays being a fully automated and low solvent technique, is also widely accepted by pharmacopoeias and regulatory agencies for use in the identification of EOs, and is also well suited to rapid metabolomic fingerprinting of multiple samples in either single or parallel runs [13]. There are further advantages of HPTLC in discovery and metabolomic studies, with compound-specific labelling and relatively low running costs [14]. Furthermore, HPTLC coupled to MS is possible for metabolomic studies of natural products [15,16].

For screening of antioxidants in natural products, the most commonly used method is the 2,2-diphenyl-1-picrylhydrazyl (DPPH·) spectrophotometric assay, based on the radical scavenging activity (RSA) of the antioxidant compounds [17]. The DPPH· assay has been widely used for measurement of the total RSA of EOs. However, without separation capability it is impossible to identify the actual components that actually provide the RSA. Thus, the coupling of the DPPH· assay and chromatographic techniques, such as high-performance liquid chromatography (HPLC) or HPTLC, have been used quite extensively for the screening of antioxidant components in natural products [17]. However, online HPLC-DPPH· methods are inappropriate for compounds (such as butylated hydroxytoluene, BHT) with slow reaction kinetics towards DPPH· [18]. In contrast, applying DPPH· as a derivatising agent with developed HPTLC plates can overcome the reaction kinetics issues with online HPLC-DPPH· methods, at the same time reducing the time and solvents required for equivalent numbers of analyses. HPTLC-DPPH· has previously been applied to the identification and determination of antioxidant compounds in EOs [19]. Identification of bioactive compounds on developed HPTLC plates can be achieved either through a visual match against a standard [20] or by subsequent analysis of bioactive bands using MS [21]. For identification of bioactive components in EOs, GC–MS or direct infusion MS (DI-MS) can also be used [19,22]. Compared to DI-MS, GC–MS provides the additional separation capability for identification of unresolved components from HPTLC.

Multivariate statistical techniques (MSTs) have found great utility in revealing the effects of genetic, environmental, and processing (extraction) variations among natural products, from within multi-dimensional data derived from their chromatographic analysis. Principal component analysis (PCA) has been used to reduce the dimensionality into two- or three-dimensional spaces through linear combination of variables in order to observe patterns among examined samples [23,24]. Partial least squares regression (PLS) is able to provide prediction of the feature of interest based on high-dimensional profiles recorded in chromatographic separation [25]. To-date HPTLC separation followed by MSTs has been applied to the discrimination of antioxidant activity in algae [26], categorisation of medical mushrooms [27] and propolis samples [28].

The main aim of this work was to discriminate YY EO samples with different distillation grades and geographical origins based on their general chemical composition (untargeted metabolomics) and RSA (targeted metabolomics) profiles. For RSA-targeted analysis, an HPTLC-DPPH· assay was used to generate a RSA-based fingerprint of antioxidant components of each YY EO sample. GC–MS and GC-FID were subsequently applied to identify the major contributors to the total RSA of YY EOs. Pearson's correlation coefficients were calculated between relative abundances and RSA of identified components to provide a correlation between quantity and bioactivity. For untargeted chemical composition analysis, classification of YY EO samples was performed based on the general chemical composition of YY EOs determined using HPTLC-ultraviolet (UV) at 254 nm and HPTLC with *p*-anisaldehyde development, followed by multivariate analysis, including PCA and PLS.

2. Experimental work

2.1. Chemicals and reagents

Dichloromethane (DCM, HPLC-grade) was purchased from Fisher Scientific (Waltham, MA, USA). Analytical grade methanol, toluene, *p*-anisaldehyde (98%), standard linear alkane mixture (C_7-C_{30}, 1000 μg mL^{-1} in hexane), ±-α-tocopherol (96%) and 2,2-diphenyl-1-picrylhydrazyl (DPPH·, 97%) were purchased from Sigma Aldrich (St. Louis, MO, USA). Glacial acetic acid (99.8%) was purchased from BDH Chemicals (Kilsyth, Australia). Sulphuric acid (≥98%) and ethyl acetate were purchased from VWR Chemicals (Radnor, PA, USA).

A mixture of toluene and ethyl acetate (95:5 v/v) was used as the developing reagent for HPTLC analysis. Preparation of 0.5% (w/v) *p*-anisaldehyde acidic alcohol solution was conducted by mixing 0.5 mL of *p*-anisaldehyde with 100 mL of prepared acidic alcohol solution (methanol/acetic acid/sulphuric acid in a mixture of 85:10:5, v/v/v). DPPH· solution (0.04%, w/v) was prepared by dissolving 40 mg of DPPH· in 100 mL of methanol and kept in the dark at 4 °C.

2.2. Sample preparation

Four grades of YY (YExtra, YI, YII, and YIII) and YCompl, comprising all grades, were obtained from Plant Therapy Inc. (Twin Falls, ID, USA) or Ahimsa Oils (Mitchelton, QLD, Australia), see Table 1. All samples for HPTLC-DPPH·, -UV and -*p*-anisaldehyde analysis were prepared by pipetting 25 μL of pure YY EO in 975 μL of DCM. EO samples from Indonesia were prepared by pipetting 50 μL of pure YY EOs in 950 μL of DCM to improve the response in HPTLC-DPPH· analysis. The underivatised HPTLC bands with RSA, aligned with the bands indicated by HPTLC-DPPH·, were scraped from a developed plate, mixed with 500 μL of DCM and extracted in an ultrasonic water bath for 10 min. After the mixture was centrifuged at a rotation speed of 10,000 rpm for 5 min, the supernatant was collected and filtered for GC–MS analysis. For GC-FID analysis, all YY EO samples were prepared by pipetting 25 μL of pure YY EO in 975 μL of DCM.

2.3. HPTLC procedure

HPTLC analysis were performed on 20 × 10 cm Merck HPTLC 60 F_{254} silica gel plates (Darmstadt, Germany) in an automatic developing chamber 2 (ADC2, CAMAG, Muttenz, Switzerland). The introduction of samples was performed at application lengths of 8 mm and distances between tracks of 11.4 mm, with a flow rate of 150 nL s^{-1}. Prior to the HPTLC development, the ADC2 was saturated for 20 min with the developing reagent. After being pre-conditioned within the vapour-saturated ADC2 for 10 min, the applied HPTLC plates were then developed with 10 mL of developing reagent to a migration distance of 80 mm. During the HPTLC development, humidity was maintained at 33% using $MgCl_2 \cdot 6H_2O$ salt in ADC2. Finally, the developed HPTLC plates were visualised under UV 254 nm, and in white light mode with remittance enhanced options using the TLC visualiser.

For RSA-targeted profiling, 1 μL of positive control tocopherol (1 mg/mL) and 1 μL of each diluted YY EO solution, was used. The developed plates were immersed in 0.04% (w/v) DPPH· solution for 5 s, dried and stored in the dark. The colouration was stabilised after 50 min and the resultant plates were used for determining the band responses.

For untargeted profiling, 3 μL of each diluted YY EO solution was applied on the plate. The developed plate was sprayed with 2 mL 0.5% (v/v) *p*-anisaldehyde reagent using a blue nozzle at level 4 in CAMAG derivatiser. The derivatised plates were developed via heating on a hot plate at 100 °C for 3 min, cooled down and visualised under white light in transmittance mode.

Table 1
List of the used samples with their codes, grade, origins and provider.

	Code	Grade	Origin	Company		Code	Grade	Origin	Company
01	YExtraMad01	Extra	Mad	PT	27	YIIIMad02	III	Mad	PT
02	YExtraMad02	Extra	Mad	PT	28	YIIIMad03	III	Mad	PT
03	YExtraMad03	Extra	Mad	PT	29	YIIIMad04	III	Mad	PT
04	YExtraMad04	Extra	Mad	PT	30	YIIIMad05	III	Mad	PT
05	YExtraMad05	Extra	Mad	PT	31	YIIIMad06	III	Mad	PT
06	YExtraNep06	Extra	Nep	PT	32	YIIIMad07	III	Mad	PT
07	YExtraCom07	Extra	Com	PT	33	YIIICom08	III	Com	PT
08	YExtraCom08	Extra	Com	AO	34	YComplMad01	Complete	Mad	PT
09	YExtraCom09	Extra	Com	AO	35	YComplMad02	Complete	Mad	PT
10	YExtraCom10	Extra	Com	AO	36	YComplMad03	Complete	Mad	PT
11	YExtraCom11	Extra	Com	AO	37	YComplMad04	Complete	Mad	PT
12	YIMad01	I	Mad	PT	38	YComplMad05	Complete	Mad	PT
13	YIMad02	I	Mad	PT	39	YComplMad06	Complete	Mad	PT
14	YIMad03	I	Mad	PT	40	YComplFra07	Complete	Fra	PT
15	YIMad04	I	Mad	PT	41	YComplAus08	Complete	Aus	AO
16	YIMad05	I	Mad	PT	42	YComplAus09	Complete	Aus	AO
17	YIMad06	I	Mad	PT	43	YComplAus10	Complete	Aus	AO
18	YICom07	I	Com	PT	44	YComplAus11	Complete	Aus	AO
19	YIFra08	I	Fra	PT	45	YComplCng12	Complete	Cng	AO
20	YIIMad01	II	Mad	PT	46	YComplCng13	Complete	Cng	AO
21	YIIMad02	II	Mad	PT	47	YComplCng14	Complete	Cng	AO
22	YIIMad03	II	Mad	PT	48	YComplCng15	Complete	Cng	AO
23	YIIMad04	II	Mad	PT	49	YComplInd16	NA	Ind	AO
24	YIICom05	II	Com	PT	50	YComplInd17	NA	Ind	AO
25	YIIFra06	II	Fra	PT	51	YComplInd18	NA	Ind	AO
26	YIIIMad01	III	Mad	PT	52	YComplInd19	NA	Ind	AO

PT: Plant Therapy Inc.; AO: Ahimsa Oils; Aus: Australia; Mad: Madagascar; Fra: France; Nep: Nepal; Com: Comoros; Cng: Congo; Ind: Indonesia; NA: Not available.

2.4. Method validation

For determination of RSA across the tested samples, the HPTLC-DPPH· assay was validated using positive control tocopherol, according to the International Conference on Harmonisation (ICH) guidelines [29]. The RSA of each radical scavenging band was expressed with tocopherol equivalence, interpolated from a tocopherol calibration curve and calculated based on each EO aliquot. Intra-plate repeatability was assessed through 5 replicates of tocopherol standard solution (2000 μg mL^{-1}), while inter-plate repeatability was determined by applying three replicates of each tocopherol standard at six different concentrations (250–8000 μg mL^{-1}). Variation among replicates was expressed as the relative standard deviation (RSD). Accuracy was assessed through calculation of the variation between interpolated concentration of tocopherol standards via the calibration curve (n = 3) and the actual concentration of tocopherol standard. Limit of detection (LOD) and limit of quantification (LOQ) were calculated by determining 3:1 and 10:1 of the signal/noise ratio, respectively.

Peak integration was performed using Origin 2018 software (OriginLab, Northampton, MA, USA). For RSA evaluation, statistical significances among different grades and geographical origins of YY EO samples were determined with one-way analysis of variance (ANOVA) followed by Tukey test using Origin. Calculated P-values were corrected to diminish false discovery rates using the Benjamini-Hochberg procedure [30].

2.5. GC–MS analysis

EO samples were analysed using a GCMS-QP2010 Plus (Shimadzu, Kyoto, Japan), equipped with a quadrupole-MS (qMS) detector. All separations were performed using a Mega-XMLB fused silica capillary column (30 m long × 0.25 mm i.d. × 0.25 μm film thickness) from BGB Analytik (Alexandria, VA, USA). The initial oven temperature was set at 80 °C and increased to 250 °C at a rate of 4.3 °C min^{-1}. The temperature was then quickly ramped (15 °C min^{-1}) to 280 °C and held constant for 5 min, resulting in a total run time of 46.5 min. Ultra-high purity helium (>99.99%) was used as carrier gas at a constant flow rate of 1.36 mL min^{-1}. The injector was set at 250 °C and sample introduction was performed by liquid injection (1 μL) of EO solution in a split mode (10:1). The ion source and transfer line temperatures were set at 220 and 250 °C, respectively. Mass fragments were recorded over the range of 40–400 amu. The acquisition rate was 5 Hz with a scan speed of 2000 amu sec^{-1}. Ionisation energy and MS detector voltages were relative to the tuning results.

Identification was performed using a similarity match (≥90%) between the experimentally obtained and the standard (library) mass spectra of the analysed compound, together with comparison of their retention indices (tolerance of ±10) with standard (library) values. The similarity search was performed using GCMS solution software (version 4.30, Shimadzu, Kyoto, Japan) within the standard libraries of the National Institute of Standards and Technology (NIST, 2005), Wiley (Wiley Registry TM of Mass Spectral Data, 11th Edition, 2016), and Flavours and Fragrances of Natural and Synthetic Compounds – Mass Spectral Database (FFNSC 2.0, 2007). Retention indices (RIs) were calculated based on the linear temperature programme retention index (LTPRI) procedure using a C_7-C_{30} standard alkane mixture, established by Van den Dool and Kratz for a temperature programmed separation [31].

2.6. GC-FID

All YY EOs were analysed with an Agilent 7890A instrument (Palo Alto, CA, USA), employing a BP5MS column, 30 m × 0.25 mm × 0.25 μm, purchased from SGE (Melbourne, Australia). The sample, 1 μL, was injected at 250 °C in split mode (20:1). The oven temperature program was set as follows: from 50 °C to 250 °C at 4.3 °C min^{-1}, and from 250 °C to 280 °C (5 min hold) at 15 °C min^{-1}. Ultra-high purity hydrogen was used as the carrier gas and the flow rate was held constant throughout the run (1.54 mL min^{-1}, linear velocity of 42.7 cm sec^{-1}). The FID detector was set at 280 °C, with a hydrogen flow of 40 mL min^{-1} and an air flow of 450 mL min^{-1}. Data processing was performed using the GC ChemStation B.0403 (16) software.

2.7. Data process

Each image of developed HPTLC plates (before and after derivatisation) for each sample was converted into a data matrix using visionCATS 2.5 software (CAMAG, Muttenz, Switzerland), along with baseline correction using a lower slope algorithm and smoothing of recorded profiles applying the Savitzky-Golay procedure with the width window set to 7 points. Negative effects of small band shifts on performance of MST were avoided by applying equidistant profile segmentation (with segment size of 0.02 R_f value).

2.8. Multivariate statistical analysis

The binned HPTLC variables, obtained by calculating the mean values of each 0.02 R_f zone, were used for multivariate statistical analysis, including PCA and PLS. As an unsupervised pattern recognition technique that is widely used for dimensionality reduction, PCA was used herein to observe clusters/patterns among different YY grades and geographical origins. Binned profiles were pre-processed using normalisation by sum and mean centring using MetaboAnalyst 4.0 online platform (www.metaboanalyst.ca) [32]. PLS was used herein to establish a cause-and-effect relationship based on a set of predictor variables (X) and response variables (Y) [23]. PLS was performed using the *mdatools* library (version 0.10.3) in R software [33]. A PLS regression model was established for the prediction of distillation grade with dummy response variables Y = 1, 2, 3, and 4, corresponding to YExtra, YI, YII, and YIII, respectively. In this way, it could be used for elucidation of the corresponding distillation grades and fragrant character of YCompl samples, which are mixtures of 4 distillation grades and do not have a specific distillation grade. This approach has already been applied for the evaluation of distillation grades of YCompl EOs based on GC–MS data [34]. Performance of the PLS model was assessed through a 10-segment double cross-validation procedure. YCompl samples from various origins, as well as YExtra samples from Comoros and Nepal, were used in double cross-validation as an independent test set. Several parameters were used to evaluate the predictive capability of the PLS model, including root mean square error of cross-validation (RMSECV), bias, standard error of prediction (SEP), and relative error of prediction (REP), as presented in Eqs. (1)–(4):

$$\mathrm{RMSECV} = \sqrt{\frac{\sum_{i=1}^{n}(C_i - C_i^{'})^2}{n}} \quad (1)$$

$$\mathrm{bias} = \frac{\sum_{i=1}^{n}(C_i - C_i^{'})}{n} \quad (2)$$

$$\mathrm{SEP} = \sqrt{\frac{\sum_{i=1}^{n}(C_i - C_i^{'} - \mathrm{bias})^2}{n-1}} \quad (3)$$

$$\mathrm{REP}(\%) = 100\sqrt{\frac{\sum_{i=1}^{n}(C_i - C_i^{'})^2}{\sum_{i=1}^{n}C_i^2}} \quad (4)$$

where C_i and $C_i^{'}$ are the actual and predicted analyte concentration in sample *i*, respectively, and *n* is the total number of samples used in the validation set [35]. The optimum number of latent variables (LVs), required for the PLS model, was determined by evaluating the lowest prediction error (RMSECV) in the validation set.

3. Results and discussion

3.1. RSA-targeted metabolomic profiling of YY EOs

3.1.1. HPTLC-DPPH· method validation

The mixture of toluene/ethyl acetate (95:5 v/v) was chosen as the developing reagent for HPTLC development, due to a high abundance of non-polar sesquiterpenes in YY EO samples, according to the literature [34]. Fig. 1a and b shows the HPTLC chromatograms visualised before (UV 254 nm) and after DPPH· derivatisation (white light). Three major discoloured bands with the retention factors (R_f) of 0.15, 0.30, and 0.66, were visualised after DPPH· derivatisation, while under UV 254 nm the major components YY EO samples were clustered in the R_f of 0.35–0.70.

A logarithmic dependence was found between the peak area of discoloured band and the tocopherol concentration in an equation of $y = 0.0034\ln(x) - 0.0179$ with a correlation coefficient (R^2) of 0.996 (Fig. S1). Intra-plate repeatability ($n = 5$) was determined with tocopherol standard solution (2000 μg mL^{-1}), resulting in an RSD of 2.84%. Inter-plate repeatability was determined with 6 different concentration levels of tocopherol standard and each level in triplicate, resulting in an RSD of 1.41–5.12% (Table S1). Accuracy ($n = 3$) between the calculated and actual concentration of tocopherol standard for 6 tocopherol concentration levels were found to be 91.48–113.68% (Table S1). LOD and LOQ of tocopherol were determined as 193.90 μg mL^{-1} and 195.34 μg mL^{-1}, respectively.

3.1.2. RSA of YY EOs

Fig. 2a and b shows the variations of the total RSA responses of YY EOs among different distillation grades (all from the same Madagascar region) and different origins, YCompl samples from Madagascar, Australia, Congo, France and Indonesia, and YExtra from Comoros and Nepal. Calculated tocopherol equivalence for all YY EOs are present in Table S2. YIII, with the longest distillation time, demonstrated the highest RSA among all distillation grades, indicating that the yield of natural antioxidants might be in proportion to the length of distillation time (Fig. 2a). The mean ± SD of the total RSAs of YY EO samples from Australia, Congo, France, Indonesia, Madagascar, Comoros and Nepal were determined to be 51.4 ± 4.3, 69.7 ± 3.3, 91.3 ± 1.7, 12.2 ± 1.4, 139.4 ± 4.9, 35.8 ± 3.7 and 43.1 ± 1.1 mg mL^{-1}, respectively.

Tables S3 and S4 showed the statistical differences of YY EO samples among different distillation grades and geographical origins. For variations of the RSA of samples classified by distillation grades, a significant difference ($p < 0.001$) was observed between YIII and YExtra and YI (Fig. 2a and Table S3), while the differences among YExtra, YI and YII, and YII and YIII were not statistically significant ($p > 0.05$). Furthermore, significant difference ($p < 0.05$) was observed in the RSA of Madagascar samples compared to samples from Australia, Comoros, Congo, Indonesia and Nepal (Fig. 2b and Table S4). No significant difference was observed in the YY EO samples among Australia, Congo, Indonesia, Comoros and Nepal. RSA of YY EOs from France were significantly different compared to those from Indonesia ($p < 0.05$).

3.1.3. Identification of RSA contributions by GC–MS and GC-FID

Fig. S2 shows the total ion current chromatograms (TICC) of three bioactive fractions, where a, b and c are corresponding to bands B1, B2 and B3 in Fig. 1b with major RSA, obtained by GC–MS. The three discoloured bands were tentatively identified using retention indices and mass spectrum data of TICC peaks, as summarised in Table S5. The major contributor to the RSA in B1 (Table S5 and Fig. S2a) was tentatively identified as linalool, which is known as a radical scavenger commonly present in EOs [36]. A mixture of eugenol and some sesquiterpenes, including β-caryophyllene, germacrene D and caryophyllene oxide, was tentatively identified in B2 (Table S5 and Fig. S2b). Eugenol has already been reported for its RSA as a natural antioxidant [37,38]. Compared to a lesser proportion of sesquiterpenes determined in B2, Fig. S2c showed a major constitution of sesquiterpenes in B3, with the most abundant ones being tentatively identified as β-caryophyllene, germacrene D and α-farnesene (Table S5 and Fig. S2c).

GC-FID was used to obtain the relative abundances of all identified compounds in each EO. The weights of contribution for the identified components in bioactive fractions to the RSA were revealed by correlating the corresponding relative abundances with RSA. Fig. S3a and S3b demonstrate the weights of contribution for the identified components

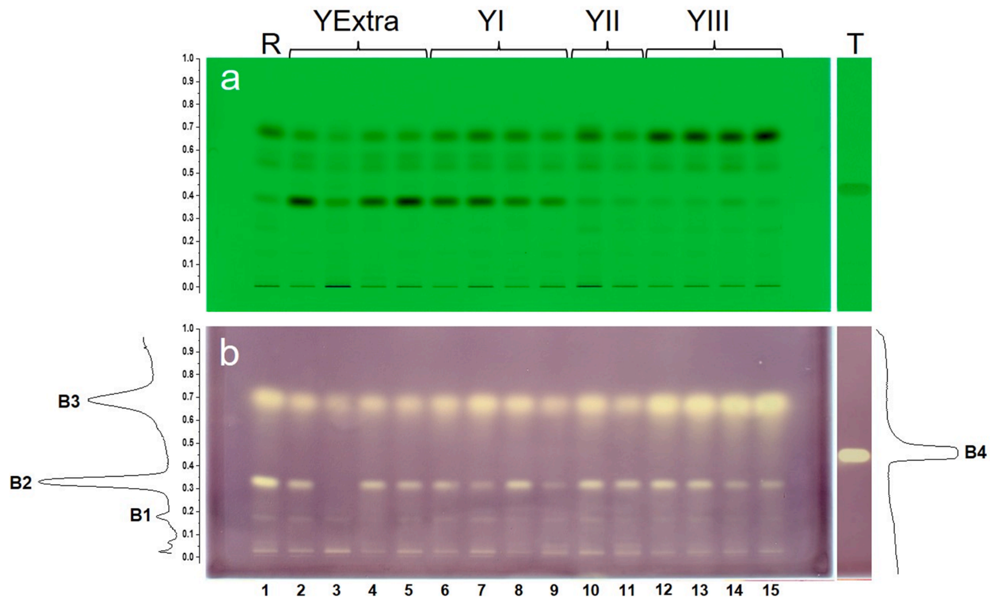

Fig. 1. HPTLC chromatogram of selected YY EOs and tocopherol visualised by view of (a) UV 254 nm, (b) Antioxidants colorised with DPPH·.

to RSA of two major bioactive fractions (corresponding to B2 and B3), expressed as Pearson's correlation coefficient, calculated between the RSA and relative abundances of analytes, obtained in GC-FID analysis, identified in bioactive fractions. Eugenol, with a Pearson's correlation coefficient of 0.81, was considered as the major contributor to the RSA of B2 among all four identified compound candidates (Fig. S3a). Fig. S3b demonstrated high Pearson's correlation coefficients for germacrene D and α-farnesene, accounting for 0.84 and 0.88, respectively. Although a high proportion of β-caryophyllene was found in B3 by GC–MS (Fig. S2c), a Pearson's correlation coefficient of −0.35 demonstrated that the RSA of B3 is not in proportion to the amount of β-caryophyllene (Fig. S3b). This agrees with the work by Noriega et al., which showed that the RSA of germacrene D is significantly higher than that of β-caryophyllene [39]. According to a previous literature [40], mono- and sesquiterpenes with multiple conjugated double-bonds are more likely to function as strong radical scavengers. Therefore, germacrene D and α-farnesene with high abundances in YY EOs are considered as the major contributors to the RSA of B3.

3.2. Metabolomic profiling of YY EOs based on HPTLC-UV and HPTLC-*p*-anisaldehyde followed by multivariate analysis

3.2.1. Pattern recognition of YY EOs using PCA

As demonstrated in Section 3.1, the RSA-based HPTLC-DPPH· fingerprint of YY EOs was used to screen the natural antioxidants and partially differentiate YY EO samples with different distillation grades and from different geographical origins. However, the discrimination power based on RSA as the only character was low. To improve the resolution for better differentiation among the YY EOs from different origins untargeted metabolomic analysis based on HPTLC-UV and HPTLC-*p*-anisaldehyde profiles was utilised. Herein, HPTLC-*p*-anisaldehyde was selected due to its suitability for most common components in YY EOs, including strong and weak nucleophiles (alcohols and amines), aldehydes and ketones [41]. For discrimination of different distillation grades of YY EOs, PCA was utilised based on the binned profiles recorded in HPTLC-UV and HPTLC-*p*-anisaldehyde analysis (as shown in Fig. S4a and S4b). Fig. 3a demonstrated a pattern for identification of the distillation grades of YY EOs, with the distribution of YExtra, YI, YII and YIII in a horizontal order from left to right. The first two principal components (PCs) for HPTLC-UV profiles explained 78.3% of the total variances (Fig. S5a). Fig. 3b showed the PCA plot for the HPTLC-*p*-anisaldehyde profiles of YY EOs. However, the PCA based on the HPTLC-*p*-anisaldehyde profiles was not suitable for discrimination of different distillation grades of YY EOs, due to a great overlap of the sample clusters, as shown in Fig. 3b.

PCA was also utilised for discrimination of different geographical origins of YY EOs based on the HPTLC-*p*-anisaldehyde profiles. Fig. 4 shows the PCA score plot including all 7 origins used in this study. In the PC 1–2 space, despite a great difference among YY EOs from Australia, Congo and Indonesia, there were only small differences among YY EOs from Nepal, Madagascar, Comoros and France, suggesting a great similarity among them in PC 1 . However, they could be separated in PC 1–3 space, which showed that the samples from 7 origins can be successfully discriminated within the first three PCs (Fig. 4). The scree plot in Fig. S6 shows how the first three PCs explained 83% of the total variances.

3.2.2. Prediction of distillation grade using PLS

It has been widely accepted that the fragrant character and price of YY EOs, and their importance for perfume and cosmetic industries, decreases in the order of the distillation grades, i.e. YExtra, YI, YII, and YIII. Also, as presented in this work, prolonged distillation time leads to samples with greater RSA, from YExtra to YIII. Therefore, grade prediction based on the profiles in HPTLC-UV analyses, is potentially of great significance to the perfume and cosmetic industries, where both fragrant character and RSA of YY EOs need to be characterised. Based on the binned HPTLC-UV profiles of those YY EOs with known distillation grades, the ranges of predicted values for YExtra, YI, YII and YIII were determined to be <1.5, 1.5–2.5, 2.5–3.5, 3.5–4.5, respectively (Table S6). The PLS prediction models were established on 2 LVs, generating a PLS regression with RMSECV of 0.365, REP = 12.9%, and $R^2 = 0.897$. Two samples, YExtraMad03 and YIIIMad05, were predicted out of the ranges for their labelled grades. Predicted grade value for the YExtraMad03 EO was 1.68, indicating that this EO is the borderline sample, and very similar to YExtraMad01, YIMad01 and YIMad02. In contrast, predicted grade value for YIIIMad05 was 3.03, which is characteristic value for the YII.

Fig. 5 depicts the distillation grade prediction of YCompl samples based on the established PLS model. All samples from Australia were classified as YII, while all samples from Comoros and Nepal were classified as YExtra, which was as per their labelled grade. One-third of samples from Madagascar were classified as YII, while the rest were classified as YI. Samples from Congo and France were classified between

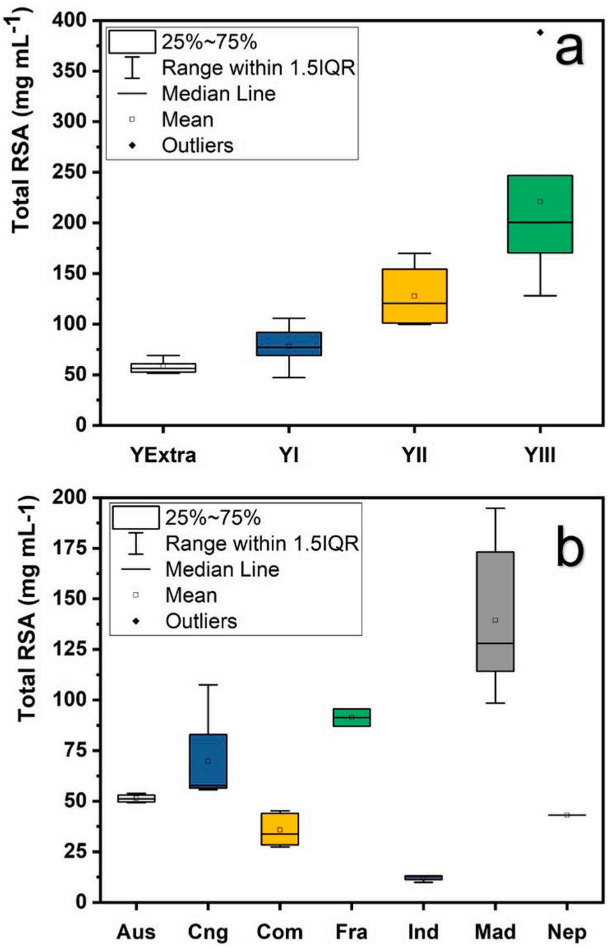

Fig. 2. Determination of total RSA (expressed as the tocopherol equivalence, in mg mL^{-1}) by HPTLC-DPPH· assay based on (a) different distillation grades of samples from Madagascar and (b) 7 different geographical origins. YY EOs from Aus, Mad, Ind, Cng and Fra are YCompl, while from Com and Nep are YExtra. (Abbreviations: Aus – Australia, Com – Comoros, Cng - Congo, Fra – France, Ind – Indonesia, Mad – Madagascar, Nep – Nepal, EO – essential oil, IQR – inter-quartile range, RSA – radical scavenging activity).

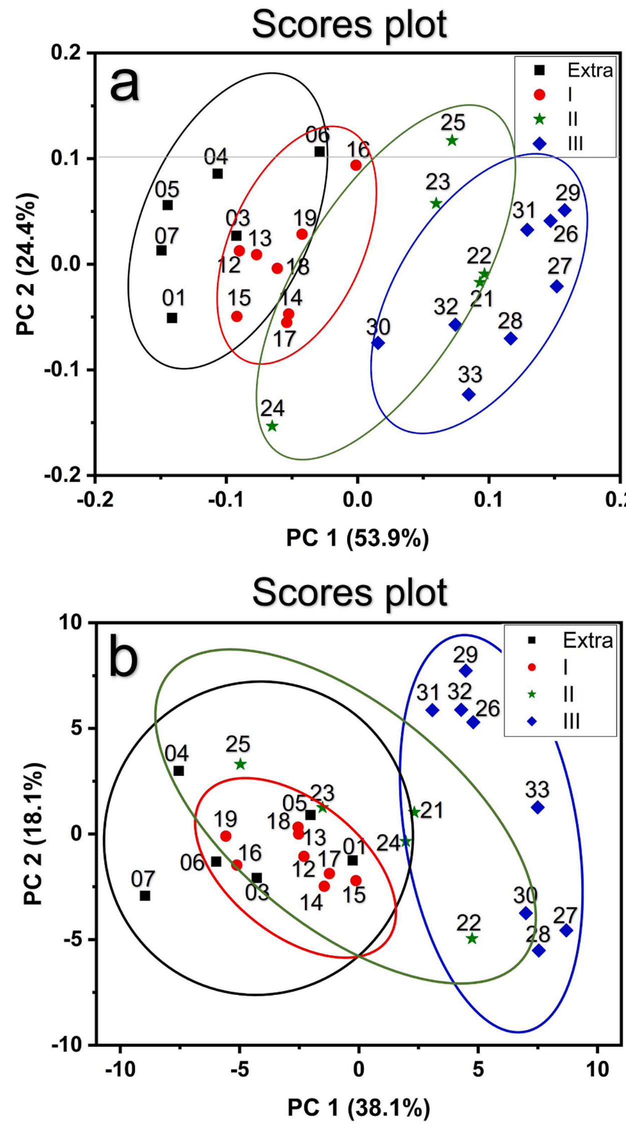

Fig. 3. PCA plots for the binned profiles recorded in (a) HPTLC-UV (visualised under UV 254 nm) and (b) HPTLC-*p*-anisaldehyde (visualised under white light) analysis.

YExtra and YI. The prediction grades, generated from the HPTLC profiles, agree with the results of a previous report from our group, where the PLS model was established based on GC–MS analysis [34].

4. Conclusion

In this study, two metabolomic profiling routes were proposed for the discrimination of 52 YY EOs with different distillation grades and geographical origins, while two different sets of information were revealed to illustrate the metabolomic profile of YY EOs. Sesquiterpenes, such as germacrene D and α-farnesene, were tentatively identified by GC–MS and GC-FID as the major RSA contributors in YY EOs, followed by eugenol and linalool as minor RSA contributors. It is demonstrated that the RSA of YY EO increased with distillation time, therefore the RSA of each separated component and fraction can be regarded as an important index for discriminating the YY EOs by distillation grades. However, it was also shown in the study that with RSA as the only character, it is difficult to classify YY EOs from specific geographical origins. Therefore, HPTLC visualisation based on the general-purpose UV absorptions and stains was used for better differentiation of YY EOs. It was demonstrated that the multi-character HPTLC profiles based on a general-purpose *p*-anisaldehyde stain produced a higher resolution PCA spectrum for discrimination of multiple YY EOs from different origins. Furthermore, a PLS model was successfully developed based on HPTLC-UV profiles, which was applied for classification of YCompl samples into specific distillation grades. As the classification of their quality and price based on distillation grades has been widely accepted in the market, it is of great importance to identify the actual distillation grade of YY EOs. The two established metabolomic fingerprint profiles provided a reference model for classification and quality evaluation of YY EOs with varying distillation grades and geographical origins.

CRediT authorship contribution statement

Leo Lebanov: Conceptualization, Investigation, Methodology, Writing - original draft. **Shing Chung Lam:** Conceptualization, Investigation, Methodology, Writing - original draft. **Laura Tedone:** Project administration, Supervision. **Tomislav Sostaric:** Conceptualization, Resources. **Jason A. Smith:** Supervision, Writing - review & editing. **Alireza Ghiasvand:** Supervision, Writing - review & editing. **Brett Paull:** Conceptualization, Supervision, Resources, Writing - review & editing.

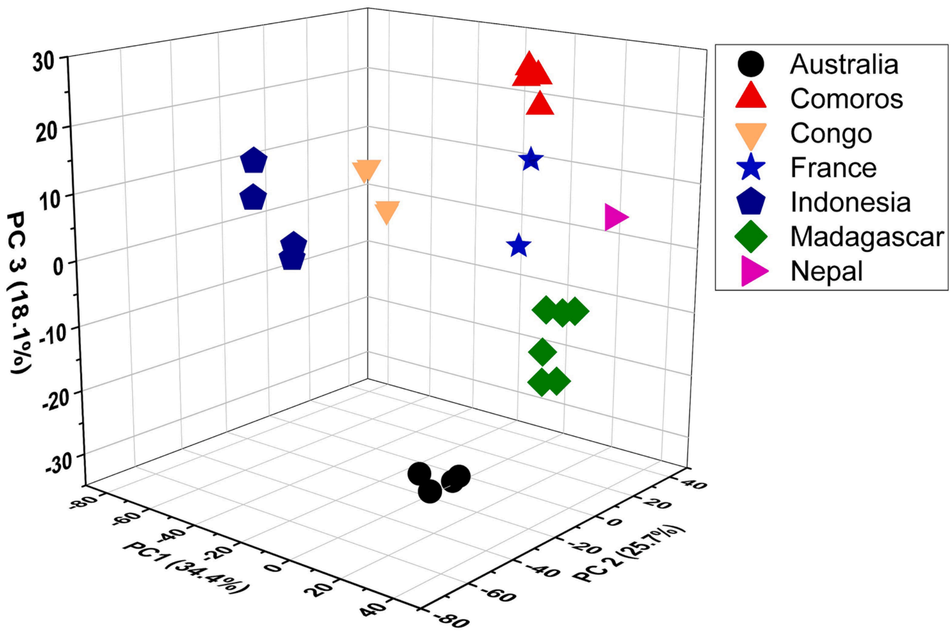

Fig. 4. 3D PCA plot for geographical origin discrimination based on the first three PCs.

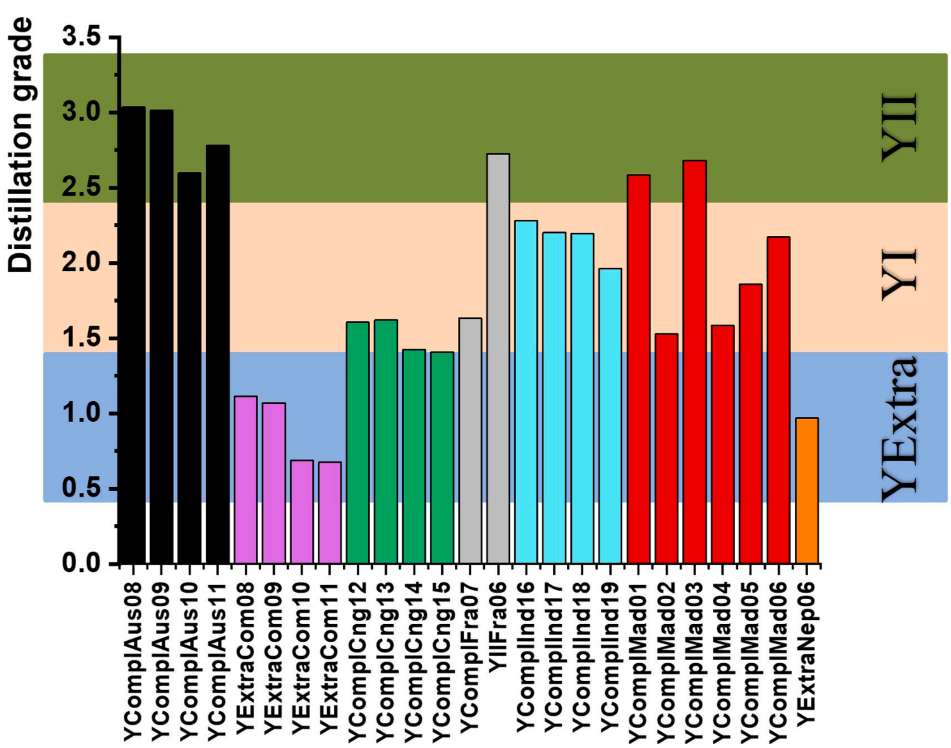

Fig. 5. Distillation grade prediction of YCompl samples based on the established PLS model.

Declaration of Competing Interest

The authors declare that they have no known competing financial interests or personal relationships that could have appeared to influence the work reported in this paper.

Acknowledgment

Authors would like to thank Plant Therapy Inc. and Ahimsa Oils for providing the essential oil samples used within this study.

Funding

This work was supported by the ARC Industrial Transformation Research Hub for Processing Advanced Lignocellulosics (PALS). Grant number: IH170100020.

Ethical approval

This article does not contain any studies with human participants or animals performed by any of the authors.

Appendix A. Supplementary material

Supplementary data to this article can be found online at https://doi.org/10.1016/j.jchromb.2021.122861.

References

[1] C. Benini, M. Ringuet, J.-P. Wathelet, G. Lognay, P. Jardin, M.-L. Fauconnier, Variations in the essential oils from ylang-ylang (Cananga odorata [Lam.] Hook f. & Thomson forma genuina) in the Western Indian Ocean islands, Flavour Fragr. J. 27 (5) (2012) 356–366, https://doi.org/10.1002/ffj.3106.

[2] L.T.H. Tan, L.H. Lee, W.F. Yin, C.K. Chan, H. Abdul Kadir, K.G. Chan, B.H. Goh, Traditional uses, phytochemistry, and bioactivities of Cananga odorata (ylang-ylang), Evid. Based Complement. Alternat. Med. 2015 (2015) 1–30, https://doi.org/10.1155/2015/896314.

[3] M. Brokl, M.L. Fauconnier, C. Benini, G. Lognay, P. du Jardin, J.F. Focant, Improvement of ylang-ylang essential oil characterization by GCxGC-TOFMS, Molecules 18 (2) (2013) 1783–1797, https://doi.org/10.3390/molecules18021783.

[4] G. Sacchetti, S. Maietti, M. Muzzoli, M. Scaglianti, S. Manfredini, M. Radice, R. Bruni, Comparative evaluation of 11 essential oils of different origin as functional antioxidants, antiradicals and antimicrobials in foods, Food Chem. 91 (4) (2005) 621–632, https://doi.org/10.1016/j.foodchem.2004.06.031.

[5] M.B. Terenina, T.A. Misharina, N.I. Krikunova, E.S. Alinkina, L.D. Fatkulina, A. K. Vorobyova, Oregano essential oil as an inhibitor of higher fatty acid oxidation, App. Biochem. Microbiol. 47 (4) (2011) 445–449, https://doi.org/10.1134/s0003683811040181.

[6] G. Ozkan, B. Simsek, H. Kuleasan, Antioxidant activities of Satureja cilicica essential oil in butter and in vitro, J. Food Eng. 79 (4) (2007) 1391–1396, https://doi.org/10.1016/j.jfoodeng.2006.04.020.

[7] M. Estévez, S. Ventanas, R. Cava, Protein oxidation in frankfurters with increasing levels of added rosemary essential oil: Effect on color and texture deterioration, J. Food Sci. 70 (7) (2005) c427–c432, https://doi.org/10.1111/jfds.2005.70.issue-710.1111/j.1365-2621.2005.tb11464.x.

[8] P. Ziosi, S. Manfredini, S. Vertuani, V. Ruscetta, M. Radice, G. Sacchetti, R. Bruni, Evaluating essential oils in cosmetics: Antioxidant capacity and functionality, Cosmetics Toiletries 125 (2010) 32–40.

[9] M.G. Miguel, Antioxidant and anti-inflammatory activities of essential oils: a short review, Molecules 15 (12) (2010) 9252–9287, https://doi.org/10.3390/molecules15129252.

[10] P.J. Marriott, R. Shellie, C. Cornwell, Gas chromatographic technologies for the analysis of essential oils, J. Chromatogr. A 936 (1-2) (2001) 1–22, https://doi.org/10.1016/S0021-9673(01)01314-0.

[11] L. Lebanov, L. Tedone, M. Kaykhaii, M.R. Linford, B. Paull, Multidimensional gas chromatography in essential oil analysis. Part 1: Technical developments, Chromatographia 82 (1) (2019) 377–398, https://doi.org/10.1007/s10337-018-3649-3.

[12] L. Lebanov, L. Tedone, M. Kaykhaii, M.R. Linford, B. Paull, Multidimensional gas chromatography in essential oil analysis. Part 2: Application to characterisation and identification, Chromatographia 82 (1) (2019) 399–414, https://doi.org/10.1007/s10337-018-3651-9.

[13] T.K.T. Do, F. Hadji-Minaglou, S. Antoniotti, X. Fernandez, Authenticity of essential oils, Trends Anal. Chem. 66 (2015) 146–157, https://doi.org/10.1016/j.trac.2014.10.007.

[14] O.L. Ogegbo, S. Eyob, S. Parmar, Z.T. Wang, S.W. Annie Bligh, Metabolomics of four TCM herbal products: Application of HPTLC analysis, Anal. Methods 4 (8) (2012) 2522–2527, https://doi.org/10.1039/c2ay25373a.

[15] E. Shawky, S.M. El Sohafy, Untargeted and targeted chemical profiling for efficacy-directed discrimination of Hedera helix L. subspecies using HPTLC- image analysis and HPTLC/MS, Ind. Crops Prod. 145 (2020) 111980, https://doi.org/10.1016/j.indcrop.2019.111980.

[16] M.N. Khanam, M. Anis, S. Ahmad, Establishment of adventitious root cultures of Allamanda cathartica L. for the production of iridoid glycosides and its identification using HPTLC MS, Ind. Crops Prod. 125 (2018) 198–206, https://doi.org/10.1016/j.indcrop.2018.08.044.

[17] S.B. Kedare, R.P. Singh, Genesis and development of DPPH method of antioxidant assay, J. Food Sci. Technol. 48 (4) (2011) 412–422, https://doi.org/10.1007/s13197-011-0251-1.

[18] I.I. Koleva, H.A.G. Niederländer, T.A. van Beek, Application of ABTS radical cation for selective on-line detection of radical scavengers in HPLC eluates, Anal. Chem. 73 (14) (2001) 3373–3381, https://doi.org/10.1021/ac0013610.

[19] J. Zhao, J.S. Zhang, B. Yang, G.P. Lv, S.P. Li, Free radical scavenging activity and characterization of sesquiterpenoids in four species of Curcuma using a TLC bioautography assay and GC-MS analysis, Molecules 15 (11) (2010) 7547–7557, https://doi.org/10.3390/molecules15117547.

[20] S.C. Lam, S.F. Lam, J. Zhao, S.P. Li, Rapid identification and comparison of compounds with antioxidant activity in Coreopsis tinctoria herbal tea by high-performance thin-layer chromatography coupled with DPPH bioautography and densitometry, J. Food Sci. 81 (9) (2016) C2218–C2223, https://doi.org/10.1111/1750-3841.13402.

[21] S.C. Lam, Z. Luo, D.T. Wu, K.L. Cheong, D.J. Hu, Z.M. Xia, J. Zhao, S.P. Li, Comparison and characterization of compounds with antioxidant activity in Lycium barbarum using high-performance thin layer chromatography coupled with DPPH bioautography and tandem mass spectrometry, J. Food Sci. 81 (6) (2016) C1378–C1384, https://doi.org/10.1111/1750-3841.13327.

[22] G. Morlock, W. Schwack, Coupling of planar chromatography to mass spectrometry, TrAC, Trends Anal. Chem. 29 (10) (2010) 1157–1171, https://doi.org/10.1016/j.trac.2010.07.010.

[23] T. Rajalahti, O.M. Kvalheim, Multivariate data analysis in pharmaceutics: A tutorial review, Int. J. Pharm. 417 (1–2) (2011) 280–290, https://doi.org/10.1016/j.ijpharm.2011.02.019.

[24] R. Bro, A.K. Smilde, Principal component analysis, Anal. Methods 6 (9) (2014) 2812–2831, https://doi.org/10.1039/c3ay41907j.

[25] K.H. Liland, Multivariate methods in metabolomics – from pre-processing to dimension reduction and statistical analysis, TrAC, Trends Anal. Chem. 30 (6) (2011) 827–841, https://doi.org/10.1016/j.trac.2011.02.007.

[26] S. Agatonovic-Kustrin, D.W. Morton, P. Ristivojevic, Assessment of antioxidant activity in Victorian marine algal extracts using high performance thin-layer chromatography and multivariate analysis, J. Chromatogr. A 1468 (2016) 228–235, https://doi.org/10.1016/j.chroma.2016.09.041.

[27] A. Bhardwaj, M. Pal, M. Srivastava, R. Tulsawani, R. Sugadev, K. Misra, HPTLC based chemometrics of medicinal mushrooms, J. Liq. Chrom. Relat. Tech. 38 (14) (2015) 1392–1406, https://doi.org/10.1080/10826076.2015.1050501.

[28] P. Ristivojević, I. Dimkić, J. Trifković, T. Berić, I. Vovk, D. Milojković-Opsenica, S. Stanković, Antimicrobial activity of Serbian propolis evaluated by means of MIC, HPTLC, bioautography and chemometrics, PLoS One 11 (6) (2016) e0157097, https://doi.org/10.1371/journal.pone.0157097.

[29] ICH, International Conference on Harmonisation, ICH Harmonized Tripartite Guidelines Q2 (R1), November 2005.

[30] Y. Benjamini, Y. Hochberg, Controlling the false discovery rate: A practical and powerful approach to multiple testing, J. R. Stat. Soc. Series B Methodol. 57 (1) (1995) 289–300, https://doi.org/10.2307/2346101.

[31] H. van Den Dool, P. Dec, Kratz, A generalization of the retention index system including linear temperature programmed gas—liquid partition chromatography, J. Chromatogr. A 11 (1963) 463–471, https://doi.org/10.1016/S0021-9673(01)80947-X.

[32] J. Chong, O. Soufan, C. Li, I. Caraus, S. Li, G. Bourque, D.S. Wishart, J. Xia, MetaboAnalyst 4.0: towards more transparent and integrative metabolomics analysis, Nucleic Acids Res. 46 (W1) (2018) 486–494, https://doi.org/10.1093/nar/gky310.

[33] S. Kucheryavskiy, mdatools: Multivariate Data Analysis for Chemometrics, R package version 0.10.3, 2017.

[34] L. Lebanov, S. Chatterjee, L. Tedone, S.C. Chapman, M.R. Linford, B. Paull, Comprehensive characterisation of ylang-ylang essential oils according to distillation time, origin, and chemical composition using a multivariate approach applied to average mass spectra and segmented average mass spectral data, J. Chromatogr. A 1618 (2020) 460853, https://doi.org/10.1016/j.chroma.2020.460853.

[35] R.R. de Oliveira, K.M. de Lima, R. Tauler, A. de Juan, Application of correlation constrained multivariate curve resolution alternating least-squares methods for determination of compounds of interest in biodiesel blends using NIR and UV-visible spectroscopic data, Talanta 125 (2014) 233–241, https://doi.org/10.1016/j.talanta.2014.02.073.

[36] H.F. Wang, K.H. Yih, K.F. Huang, Comparative study of the antioxidant activity of forty-five commonly used essential oils and their potential active components, J. Food Drug Anal. 18 (1) (2010) 24–33, https://doi.org/10.38212/2224-6614.2225.

[37] R. Amorati, M.C. Foti, L. Valgimigli, Antioxidant activity of essential oils, J. Agric. Food. Chem. 61 (46) (2013) 10835–10847, https://doi.org/10.1021/jf403496k.

[38] H.F. Wang, K.H. Yih, C.H. Yang, K.F. Huang, Anti-oxidant activity and major chemical component analyses of twenty-six commercially available essential oils, J. Food Drug Anal. 25 (4) (2017) 881–889, https://doi.org/10.1016/j.jfda.2017.05.007.

[39] P. Noriega, A. Guerrini, G. Sacchetti, A. Grandini, E. Ankuash, S. Manfredini, Chemical composition and biological activity of five essential oils from the Ecuadorian Amazon rain forest, Molecules 24 (8) (2019) 1637, https://doi.org/10.3390/molecules24081637.

[40] C.E. Vickers, J. Gershenzon, M.T. Lerdau, F. Loreto, A unified mechanism of action for volatile isoprenoids in plant abiotic stress, Nat. Chem. Biol. 5 (5) (2009) 283–291, https://doi.org/10.1038/nchembio.158.

[41] S. Agatonovic-Kustrin, E. Kustrin, V. Gegechkori, D.W. Morton, High-performance thin-layer chromatography hyphenated with microchemical and biochemical derivatizations in bioactivity profiling of marine species, Mar. Drugs 17 (3) (2019) 148, https://doi.org/10.3390/md17030148.